Activity-associated effect of LDL receptor missense variants located in the cysteine-rich repeats

A. Etxebarria[1#], A. Benito-Vicente[1#], M. Stef[2], H. Ostolaza[1], L. Palacios[2], C. Martin[1*]

[1]Unidad de Biofísica (CSIC, UPV/EHU) and Departamento de Bioquímica, Universidad del País Vasco, Apdo. 644, 48080 Bilbao, Spain.

[2] Progenika Biopharma, a Grifols Company, Derio, Spain.

[*] Corresponding Author E-mail: cesar.martin@ehu.es. Tel. +34-94-601.80.53; Fax +34-94-601.33.60

[#] A.E. and A.B-V. have equally contributed to this work

Number of Tables: 2

Number of Figures: 7

Number of supplementary Figures: 6

Number of supplementary Tables: 1

Abstract

Background: The LDL receptor (LDLR) is a Class I transmembrane protein critical for the clearance of cholesterol-containing lipoprotein particles. The N-terminal domain of the LDLR harbours the ligand-binding domain consisting of seven cysteine-rich repeats of approximately 40 amino acids each. Mutations in the *LDLR* binding domain may result in loss of receptor activity leading to familial hypercholesterolemia (FH). In this study the activity of six mutations located in the cysteine-rich repeats of the *LDLR* has been investigated.

Methods: CHO-*ldlA7* transfected cells with six different *LDLR* mutations have been used to analyse *in vitro* LDLR expression, lipoprotein binding and uptake. Immunoblotting of cell extracts, flow cytometry and confocal microscopy have been performed to determine the effects of these mutations. *In silico* analysis was also performed to predict the mutation effect.

Results and conclusion: From the six mutations, p.Arg257Trp turned out to be a non-pathogenic LDLR variant whereas p.Cys116Arg, p.Asp168Asn, p.Asp172Asn, p.Arg300Gly and p.Asp301Gly were classified as binding-defective LDLR variants whose effect is not as severe as null allele mutations.

Keywords: LDLR, mutations, Familial hypercholesterolemia, ligand binding domain, mutation Class defect

1. Introduction

Familial Hypercholesterolemia (FH; MIM#143890) is an autosomal dominant disorder causing premature coronary heart disease (CHD) [1] that is characterized by increased plasma LDL cholesterol, tendon xanthomas, deposits of cholesterol in peripheral tissues and accelerated atherosclerosis. FH has a homozygous frequency of 1:1,000,000, and its heterozygous frequency has recently been estimated to be as high as 1/200 in the general population [2,3], suggesting that the disease is heavily underdiagnosed and undertreated. FH is mainly due to mutations in the LDL receptor (LDLR; MIM# 606945) gene, which is responsible for the uptake of LDL particles into cells [1].

The LDLR is a modular protein that combines five different domains: the ligand binding domain, the EGF-like module that contain a 280 amino acid β-propeller, the O-glycosylated domain and the transmembrane and cytoplasmic domains. The binding domain of LDLR comprises ~40-amino acid long cysteine-rich repeats in tandem, structured in seven discrete extracellular modules (R1-R7), which are responsible for the binding and release of its lipoprotein ligands [4]. After binding, the LDLR-lipoprotein complex is internalized through clathrin-coated pits and traffics to endosomes, where lipoprotein cargo is released [5,6]. Lipoproteins are subsequently degraded in lysosomes, while the LDLR recycles back to the cell surface for further rounds of lipoprotein uptake. Nowadays more than 1300 different variants have been described in the LDLR gene [7], not all of them pathogenic. According to the nature and location of the mutations within the *LDLR* and to the phenotypic effects on the protein, mutations have been divided into five different classes [8]: Class 1: no detectable LDLR synthesis; Class 2: defective LDLR transport; Class 3: impaired LDL to LDLR binding; Class 4: no LDLR/LDL internalization due to defective clustering in clathrin-coated pits; and Class 5: no LDLR recycling.

The fact that several missense variants of the *LDLR* found in FH patients have been shown not to be the actual cause of the disease [9,10] indicates that every detected variant needs to be functionally characterized in order to determine its severity, if any. The aim of this study was to analyse the impact on the LDLR activity of six missense variants located in the ligand binding domain of the protein, and previously found in FH patients. The sequence variations studied predict the following amino acid changes in the LDLR: p.Cys116Arg, p.Asp168Asn, p.Asp172Asn, p.Arg257Trp, p.Arg300Gly and p.Asp301Gly. The effects on LDLR expression, binding capacity and uptake were studied by Western blot, flow cytometry and confocal microscopy in a transfected *LDLR*-defective Chinese hamster ovary (CHO) cell line.

2. Materials and Methods

2.1. Selection of Variants

The selection of the six missense *LDLR* variants was based on two criteria: to have been previously found in FH patients and to be possibly associated to a binding defect. To cover the first criteria we selected variants previously described by other authors in FH patients that have also been found in at least one FH index case by LIPOchip® platform [11] or by SEQPRO LIPO RS® platform in Progenika Biopharma (Derio, Spain), both platforms with the CE mark. Just two of the variants have been found in large population studies, p.Asp168Asn and p.Arg257Trp, that were coded as rs200727689 and rs200990725, respectively in the NCBI SNP database (http://www.ncbi.nlm.nih.gov/projects/SNP/snp_ref.cgi?geneId=3949). Both of them have a very low frequency, p.Asp168Asn has been found in the EVS database (http://evs.gs.washington.edu/EVS/) with a MAF(%)= 0.0154 and p.Arg257Trp in the 1000 genomes database (http://browser.1000genomes.org.) with a MAF(%)=0.001. The characteristics of the selected variants are compiled in Table 1 and their location within

the protein is shown in Figure 1.

2.2. Site-directed mutagenesis

Plasmids carrying the *LDLR* variants were constructed by Innoprot (Derio, Spain) as described in Online Supp. Data.

2.3. Cell culture and transfection

LDLR-deficient CHO cell line *ldl*A7 (CHO-*ldl*A7) (kindly provided by Dr. Monty Krieger, Massachusetts Institute of Technology, Cambridge, MA) was cultured in Ham's F-12 medium supplemented with 5% FBS, 2 mM L-glutamine, 100 units/mL penicillin, and 100 µg/mL streptomycin. CHO-*ldl*A7 cells were plated into 6- or 24-well culture plates, and transfected with plasmids carrying the *LDLR* variants using Lipofectamine® LTX and Plus™ Reagent (Invitrogen) according to the manufacturer's instructions. Transfected cells were maintained in culture during 48 h to achieve maximal LDLR expression.

2.4. Western blot analysis

Cell lysates were prepared, protein concentration determined, and fractionated by electrophoresis as described in Online Supp. Data.

2.5. Lipoprotein isolation

LDL and VLDL were isolated from blood samples of healthy individuals in a two step centrifugation as described in Online Supp. Data.

2.6. Lipoprotein labelling

LDL and VLDL were labelled with FITC as previously described [12]. Briefly, lipoproteins (1mg/mL) in 0.1 M $NaHCO_3$ (pH 9.0) was mixed with 10 µl/mL FITC (2 mg/mL in dimethyl sulfoxide). The mixture was gently mixed by slow rocking at room temperature for 2 h. The unreacted dye was removed by gel filtration on a Sephadex G-25 column equilibrated with PBS EDTA-free buffer. All fractions were assayed for

protein content with bovine serum albumin as standard (Pierce BCA protein assay, Pierce).

2.7. Quantification of LDLR activity by flow cytometry

Transfected CHO-*ldl*A7 cells were grown in 24-well culture plates. 48 h after transfection, cells were incubated for 4 h, at 37ºC or at 4ºC with 20 µg/mL FITC-LDL to determine LDLR activity or LDL-LDLR binding, respectively. After incubation with FITC-LDL, CHO-*ldl*A7 cells were washed twice in PBS-1%BSA, fixed on 4% formaldehyde for 10 min and washed again twice with PBS-1%BSA. To determine the amount of internalized LDL, Trypan blue solution (Sigma-Aldrich, Steinheim, Germany) was added directly to the samples to a final concentration of 0.2%, eliminating the extracellular signal due to the non-internalized LDL-LDLR complexes. Measurement of VLDL was performed by incubation of cells with 20 µg/mL FITC-VLDL for 4 h, at 37ºC as described for LDL. Fluorescence intensities were measured by FACS, in a Facscalibur Flow cytometer according to the manufacturer instructions as previously described [9]. For each sample, fluorescence of 10,000 events was acquired for data analysis. All measurements were performed at least in triplicate.

2.8. Quantification of LDLR expression by flow cytometry

To determine LDLR cell surface expression by FACS, transfected CHO-*ldl*A7 cells grown during 48 h were incubated with a mouse primary antibody anti-LDLR (1:100; 2.5 mg/L; Progen Biotechnik GmbH) for 1 h, at room temperature, then washed twice with PBS-1%BSA and incubated with secondary antibody Alexa Fluor 488-conjugated goat anti-mouse IgG (1:100; Molecular Probes). For each sample, fluorescence of 10,000 events was acquired for data analysis. All measurements were performed at least in triplicate.

2.9. Confocal Laser Scanning Microscopy (CLSM)

CLSM was used to analyse LDL-LDLR binding and LDL uptake in *LDLR* transfected CHO-*ldl*A7 cells. Briefly, cells were plated in coverslips and then transfected with the *LDLR* containing plasmids and cultured for 48 h, at 37ºC in 5% CO_2. Then the medium was removed and coverslips washed twice with PBS-1%BSA. To determine LDL-LDLR binding and LDL uptake, non-labelled lipoproteins (20 µg/mL LDL) were added and cells were incubated for additional 4 h at 4ºC or 37ºC, respectively. Cells were fixed with 4% paraformaldehyde during 10 min, washed three times with PBS-1%BSA and permeabilised with 1% Triton X-100 for 30 min at room temperature. Samples were then washed and blocked in PBS-10%FBS for 1 h and washed in PBS-1%BSA three times. Then samples were incubated with the appropriate primary antibodies for 16 h at 4ºC, followed by incubation with the appropriate fluorescent secondary antibodies. Coverslips were mounted on a glass slide and samples were visualised using a confocal microscope (Olympus IX 81) with sequential excitation and capture image acquisition with a digital camera (Axiocam NRc5, Zeiss). Images were processed with Fluoview v.50 software. Image analysis to quantify the fluorescence intensities was accomplished using the public domain software ImageJ (available at http://rsb.info.nih.gov/ij) running on a standard PC.

2.10. *In silico* predicted effect of molecular event on LDLR

The possible impact of amino acid substitutions on the structure and function of missense variants was predicted by using four different softwares as described in Online Supp. Data.

2.11. Conservation analysis

Conservation analysis among species for nucleotide and amino acid was carried out as described in Online Supp. Data.

2.12. Statistical analysis

All measurements were performed at least 3 times, with n=3 unless otherwise stated,

and results are presented as mean ± s.d. Levels of significance were determined by a two-tailed Student's t-test, and a confidence level of greater than 95% ($p<0.05$) was used to establish statistical significance.

3. Results

3.1. *In silico* analysis

The results obtained by different software packages are presented in Table 2. Depending on the program, especially Align GVGD compared to the other ones, the prediction of the effect caused by the variants is different. All the variants except p.Arg257Trp and p.Arg300Gly were classified as pathogenic by the majority of the prediction programs. These 2 variants are the less conserved ones and, as the prediction algorithms are mainly based on conservation analysis, the results are the expected ones. No splicing defects were predicted for any of the studied variants (data not shown).

3.2. Expression of LDLR variants in CHO-*ldl*A7 cells

CHO-*ldl*A7 cells were transfected with plasmids carrying the different variants and LDLR expression was assayed by immunoblotting as described in *Materials and Methods*. As shown in Figure 2A (upper panel), all the mutated LDLR are expressed at similar levels as wt 48 h after transfection. Equal loading of protein was confirmed in each blot by membrane stripping and further incubation with antibodies to visualise cytosolic GAPDH protein (Figure 2A, lower panel). The extent of protein expression was determined by quantitative densitometric analysis (Figure 2B). The data obtained by flow cytometry confirmed these results, the LDLR expression of all the variants being similar to the one in the wt (Figure 3A).

3.3. Analysis of LDLR activity by FACS

CHO-*ldl*A7 cells expressing wt LDL receptor or LDLR p.Cys116Arg, p. Asp168Ans, p.Asp172Asn, p.Arg257Trp, p.Arg300Gly and p.Asp301Gly variants were assayed for

LDL binding and uptake by flow cytometry. For internal method validation two controls were used because their effects on expression, binding and uptake are optimal for comparison with the experimental results obtained by FACS. One of the control is p.Trp87*, a null allele mutant, that does not produce LDLR. The other internal control is Ex3_4del mutant that produces a defective binding protein because the mRNA contains an in frame deletion of exons 3 and 4, essential for LDL binding [13]. As shown in Figure 3B, LDL-LDLR binding activities were similar in wt and p.Arg257Trp. However, binding activities of the other 5 variants were diminished as compared to wt (Figure 3B). As shown in Figure 3C and in agreement with LDLR expression and binding results, LDL internalisation in p.Arg257Trp was similar to wt, and LDL uptake determined in the other 5 variants was diminished when compared to wt. Values of LDLR expression, LDL binding and LDL uptake are shown in Supplementary Table 1.

3.4. Analysis of LDLR activity by confocal microscopy

Confocal microscopy was used to confirm the activities and phenotypes of the analysed LDLR variants. CHO-*ldl*A7 cells expressing either wt or the LDLR variants were incubated with LDL for 4 h and then immunostained with the appropriate antibodies to determine LDLR and LDL localisation within the cell. LDL incubation was performed at 4ºC to determine LDL binding, or at 37ºC to determine LDL uptake. FITC or Texas Red® -conjugated secondary antibodies were used to visualise LDLR and LDL respectively. Figures S1 and S2 show LDL binding to CHO-*ldl*A7 transfected cells at low magnification in order to show a wide field with multiple cells. As shown in Figure 4A, LDLR expression and LDL binding, determined at 4ºC, were similar in wt and in p.Arg257Trp. Quantification of fluorescence intensities of the images obtained by confocal microscopy showed no statistically significant differences between wt and p.Arg257Trp (Figure 4C upper: LDL expression, and Figure 4C middle: LDL binding).

Similarly to the obtained results by FACS, LDL uptake determined by confocal microscopy for p.Arg257Trp was similar to wt (Figure 4B). Quantification of fluorescence intensities of confocal images corroborated the similar uptake determined by FACS both in wt and p.Arg257Trp (Fig 4C, lower panel).

Confocal microscopy was also used to confirm the results of the five pathogenic variants determined by FACS. Figure 5A shows LDLR expression and LDL binding of p.Cys116Arg, p.Asp168Asn, p.Asp172Asn, p.Arg300Gly and p.Asp301Gly determined at 4ºC. The images confirm that LDLR expression is similar in all of them compared to wt and that in all cases the LDLR reaches the membrane and it is not retained in the ER. However looking at LDL binding, it is evident that LDL binding to the five pathogenic LDLR is largely diminished. Quantification of the images fluorescence intensities showed statistically significant differences in LDL binding between wt and the pathogenic LDLRs for LDLR expression (Figure 5B). In agreement with the FACS results LDL uptake determined by confocal microscopy for these pathogenic LDLRs was lower compared to wt (Figure 6A). Quantification of LDL uptake from the fluorescence intensities of the confocal images shown in Figure 6B confirms the results obtained by FACS.

According to the above results p.Arg257Trp can be classified as a non pathogenic LDLR variant, whereas p.Cys116Arg, p.Asp168Asn, p.Asp172Asn, p.Arg300Gly and p.Asp301Gly belong to the pathogenic Class 3 type, since ligand binding is impaired. Although the 5 variants affect LDLR activity, none of them is as severe as a null allele. Values of LDLR expression, LDL binding and LDL uptake are shown in Supplementary Table 1.

3.5. Analysis of VLDL uptake by FACS

VLDL uptake by CHO-*ldl*A7 cells expressing either the wt LDL receptor or the six LDLR variants was assayed to analyse if these amino acid substitutions impair the receptor capacity to bind VLDL. In this assay, Ex3_4del mutant was also used as internal control because it lacks the R4 module which together with R5 are the key modules for VLDL binding. As expected, VLDL uptake was significantly reduced as compared to wt LDLR. As shown in Figure 7, VLDL uptake in the variants containing amino acid substitutions in modules R3 or R4 was significantly decreased when compared to wt, whereas amino acid substitution in modules R6 or R7 did not affect VLDL uptake as compared to wt LDLR (Figure 7).

4. Discussion

LDLR is a Class I transmembrane glycoprotein whose primary role is to remove cholesterol-rich lipoprotein particles from blood circulation [5]. The receptor exhibits high-affinity binding both to LDL particles [14], which contain a single copy of apolipoprotein B-100 (apoB-100), and to VLDL particles [15], containing multiple copies of apolipoprotein E (apoE). The binding domain of LDLR to lipoproteins comprises seven tandemly repeated cystein rich domains called R1-R7 (Figure 1) [16]. Each repeat is composed of about 40 amino acids and contains two loops stabilized by three disulphide bridges. Each coordinates with one Ca^{2+} ion allowing the correct folding of the modules, which is required for lipoprotein binding at 1:1 stoichiometry [17]. The most important physiological ligand for the receptor is LDL, which contains a single copy of apoB-100, but LDLR has also the capacity to bind lipoproteins that contain apoE [13,15,18].

In this study we have analysed the activity of six *LDLR* variants, located in the binding domain of the receptor, in CHO-*ldl*A7 transfected cells which mimic the effect of these variants in homozygous form. Data of LDL binding and uptake show that p.Arg257Trp

is a non-pathogenic variant, while the other five can be classified as pathogenic class 3 variants since they have diminished LDL binding activities. The ~40-50% reduced activity found in p.Cys116Arg, p.Asp168Asn, p.Asp172Asn, p.Arg300Gly and p.Asp301Gly variants suggests that these mutations would be more benign than others in which binding or internalization are more severely impaired and might be expected to lead to less severe hypercholesterolaemia. Hence the lipid profile would not reflect the presence of FH thus leading to an incorrect diagnosis of patients in whom the phenotype has not already developed.

The mutations characterized in this work also display a differential impact on LDL *vs* VLDL uptake depending on the localization of the mutation. VLDL uptake in p.Arg257Trp, p.Arg300Gly and p.Asp301Gly variants is similar to that of wt, however, p.Cys116Arg, p.Asp168Asn, p.Asp172Asn variants show ~50% reduced VLDL uptake as compared to wt. The very low density lipoprotein receptor (VLDLR), LDLR, and low density lipoprotein receptor-related protein (LRP) are the three main apoE-recognizing endocytic receptors involved in the clearance of triglyceride (TG)-rich lipoproteins from plasma [19]. It has been previously shown that LDLR deficiency in mice results in moderate accumulation of plasma TG-rich lipoproteins when TG metabolism is stressed either by a high-fat diet or on a background of obesity [20,21]. In humans the extents to which VLDL and IDL are cleared from plasma by LDL receptors *in vivo* are not clearly established, although the normal plasma triglyceride levels found in FH patients suggest that the LDLR plays a major role in the clearance of LDL, but not of VLDL or IDL. It is possible that the impaired VLDL uptake in p.Cys116Arg, p.Asp168Asn, or p.Asp172Asn variants could result in moderate accumulation of plasma TG-rich lipoproteins not compensated by the presence in the peripheral tissues of VLDLR and LRP. Therefore, a detailed study of the lipid profiles

of patients together with the functional characterization of mutations within the LDLR binding domain would be necessary to gain insight of the role of LDLR in the clearance of VLDL, TG-rich VLDL, VLDL remnants, and IDL in humans.

It is also remarkable that none of the four prediction programs used have had a 100% of accuracy in predicting pathogenicity. This lack of effectiveness may be due to the fact that *in silico* analyses are based on the amino acid conservation and they do not consider either the consequences of missense variants on the structure of the R modules or the interaction of the LDLR protein with the LDL. However, considering the function of a given amino acid, structure or interactions contributes to understand the impact of missense mutations on protein function and may thereby ensure a better fit between *in silico* and *in vitro* data. For example, the p.Cys116Arg variant resides in the R3 module of the binding domain; this amino acid substitution disrupts a disulphide bond that maintains the structure of this module (Figure S3). Hence, the cause of the impaired functionality of the whole module may reside in the incorrect folding of the receptor. In the case of p.Asp168Asn and p.Asp172Asn, the required calcium binding of the R4 module (Figures S4 and S5) is affected, resulting in an impaired LDL binding capacity of ~65% compared to wt. The same effects are observed when looking at VLDL uptake that show experimental higher uptake capacities than the theoretically expected one in a totally R4 non functional LDLR. Finally, p.Asn300Gly and p.Asp301Gly are two mutations located in the R7 module (Figure S6), the results of LDLR binding and uptake activities show that both mutations fail to bind LDL but retain an intact capacity to bind VLDL. Asp301 is one of the residues responsible for Ca^{2+} binding to R7 module. Therefore, Asp replacement by a Gly may result in a partially or totally unstructured module that explains the diminished LDL binding of this receptor. Asn300 is not directly involved in calcium coordination but could give some steric restrictions to the

module facilitating an optimal conformation for a correct calcium binding. However, a glycine substitution at this location by diminishing the imposed steric restrictions could prevent the correct folding of R7.

In conclusion, this work demonstrates the effect of six variants located in the LDLR ligand binding domain and their consequences on the LDLR activity, and it highlights the importance of understanding the pathogenicity of these variants. The data will help clinicians to interpret FH genetic diagnosis, particularly when the LDLR activity is partially reduced and the clinical diagnosis in heterozygosis is more difficult, in case of finding any of the pathogenic variants to carry out cascade screening, and in case of finding p.Arg257Trp to discard it as the possible FH cause. It is important to note that the two studied missense mutations occurring in R7, although affecting LDL binding and uptake, do not affect VLDL uptake. This reveals that the conformational change occurring in the module does not propagate to the whole ligand binding domain.

Acknowledgements

Technical and human support provided by SGIker (Analytical and High-Resolution Microscopy in Biomedicine Service of the UPV/EHU) and Rocío Alonso for excellent technical assistance are gratefully acknowledged. We thank Prof. A. Gómez-Muñoz for flow cytometry facilities, and Dr. Monty Krieger for kindly providing *CHO-ldlA7* cells. We sincerely thank Professsor Félix M. Goñi and Dr. Ana Cenarro for their critical reading of this manuscript. This work was supported by the Spanish Ministry of Economy and Competitiveness, Programa INNPACTO (grant Nº IPT-2011-0817-010000) and from the Spanish Ministerio de Ciencia y Tecnología (Project BFU 2012-36241), and the Basque Government (Grupos Consolidados IT849-13 and ETORTEK Program).

References

1. Goldstein JL HH, Brown MS (2001) Familial hypercholesterolemia; C.R. Scriver ALB, W.S. Sly and D. Valle, Editors, editor. New York McGraw-Hill.
2. Benn M, Watts GF, Tybjaerg-Hansen A, Nordestgaard BG (2012) Familial hypercholesterolemia in the danish general population: prevalence, coronary artery disease, and cholesterol-lowering medication. J Clin Endocrinol Metab 97: 3956-3964.
3. Nordestgaard BG, Chapman MJ, Humphries SE, Ginsberg HN, Masana L, et al. (2013) Familial hypercholesterolaemia is underdiagnosed and undertreated in the general population: guidance for clinicians to prevent coronary heart disease: consensus statement of the European Atherosclerosis Society. Eur Heart J 34: 3478-3490a.
4. Yamamoto T, Davis CG, Brown MS, Schneider WJ, Casey ML, et al. (1984) The human LDL receptor: a cysteine-rich protein with multiple Alu sequences in its mRNA. Cell 39: 27-38.
5. Brown MS, Goldstein JL (1986) A receptor-mediated pathway for cholesterol homeostasis. Science 232: 34-47.
6. Rudenko G, Henry L, Henderson K, Ichtchenko K, Brown MS, et al. (2002) Structure of the LDL receptor extracellular domain at endosomal pH. Science 298: 2353-2358.
7. Leigh SE, Foster AH, Whittall RA, Hubbart CS, Humphries SE (2008) Update and analysis of the University College London low density lipoprotein receptor familial hypercholesterolemia database. Ann Hum Genet 72: 485-498.
8. Hobbs HH, Russell DW, Brown MS, Goldstein JL (1990) The LDL receptor locus in familial hypercholesterolemia: mutational analysis of a membrane protein. Annu Rev Genet 24: 133-170.
9. Etxebarria A, Palacios L, Stef M, Tejedor D, Uribe KB, et al. (2012) Functional characterization of splicing and ligand-binding domain variants in the LDL receptor. Hum Mutat 33: 232-243.
10. Huijgen R, Kindt I, Fouchier SW, Defesche JC, Hutten BA, et al. (2010) Functionality of sequence variants in the genes coding for the low-density lipoprotein receptor and apolipoprotein B in individuals with inherited hypercholesterolemia. Hum Mutat 31: 752-760.
11. Palacios L, Grandoso L, Cuevas N, Olano-Martin E, Martinez A, et al. (2012) Molecular characterization of familial hypercholesterolemia in Spain. Atherosclerosis 221: 137-142.
12. Dardik R, Varon D, Tamarin I, Zivelin A, Salomon O, et al. (2000) Homocysteine and oxidized low density lipoprotein enhanced platelet adhesion to endothelial cells under flow conditions: distinct mechanisms of thrombogenic modulation. Thromb Haemost 83: 338-344.
13. Esser V, Limbird LE, Brown MS, Goldstein JL, Russell DW (1988) Mutational analysis of the ligand binding domain of the low density lipoprotein receptor. J Biol Chem 263: 13282-13290.
14. Goldstein JL, Brown MS (1974) Binding and degradation of low density lipoproteins by cultured human fibroblasts. Comparison of cells from a normal subject and from a patient with homozygous familial hypercholesterolemia. J Biol Chem 249: 5153-5162.
15. Innerarity TL, Mahley RW (1978) Enhanced binding by cultured human fibroblasts of apo-E-containing lipoproteins as compared with low density lipoproteins. Biochemistry 17: 1440-1447.

16. Fass D, Blacklow S, Kim PS, Berger JM (1997) Molecular basis of familial hypercholesterolaemia from structure of LDL receptor module. Nature 388: 691-693.
17. Van Driel IR, Brown MS, Goldstein JL (1989) Stoichiometric binding of low density lipoprotein (LDL) and monoclonal antibodies to LDL receptors in a solid phase assay. J Biol Chem 264: 9533-9538.
18. Jeon H, Blacklow SC (2005) Structure and physiologic function of the low-density lipoprotein receptor. Annu Rev Biochem 74: 535-562.
19. Espirito Santo SM, Rensen PC, Goudriaan JR, Bensadoun A, Bovenschen N, et al. (2005) Triglyceride-rich lipoprotein metabolism in unique VLDL receptor, LDL receptor, and LRP triple-deficient mice. J Lipid Res 46: 1097-1102.
20. Goudriaan JR, Tacken PJ, Dahlmans VE, Gijbels MJ, van Dijk KW, et al. (2001) Protection from obesity in mice lacking the VLDL receptor. Arterioscler Thromb Vasc Biol 21: 1488-1493.
21. Tacken PJ, Teusink B, Jong MC, Harats D, Havekes LM, et al. (2000) LDL receptor deficiency unmasks altered VLDL triglyceride metabolism in VLDL receptor transgenic and knockout mice. J Lipid Res 41: 2055-2062.
22. Marduel M, Carrie A, Sassolas A, Devillers M, Carreau V, et al. (2010) Molecular spectrum of autosomal dominant hypercholesterolemia in France. Hum Mutat 31: E1811-1824.
23. Tosi I, Toledo-Leiva P, Neuwirth C, Naoumova RP, Soutar AK (2007) Genetic defects causing familial hypercholesterolaemia: identification of deletions and duplications in the LDL-receptor gene and summary of all mutations found in patients attending the Hammersmith Hospital Lipid Clinic. Atherosclerosis 194: 102-111.
24. Cenarro A, Jensen HK, Casao E, Civeira F, Gonzalez-Bonillo J, et al. (1998) Identification of recurrent and novel mutations in the LDL receptor gene in Spanish patients with familial hypercholesterolemia. Mutations in brief no. 135. Online. Hum Mutat 11: 413.
25. Day IN, Whittall RA, O'Dell SD, Haddad L, Bolla MK, et al. (1997) Spectrum of LDL receptor gene mutations in heterozygous familial hypercholesterolemia. Hum Mutat 10: 116-127.
26. Jensen JM, Kruse TA, Brorholt-Petersen JU, Christiansen TM, Jensen HK, et al. (1999) Linking genotype to aorto-coronary atherosclerosis: a model using familial hypercholesterolemia and aorto-coronary calcification. Ann Hum Genet 63: 511-520.
27. Nauck MS, Koster W, Dorfer K, Eckes J, Scharnagl H, et al. (2001) Identification of recurrent and novel mutations in the LDL receptor gene in German patients with familial hypercholesterolemia. Hum Mutat 18: 165-166.
28. Santos PC, Morgan AC, Jannes CE, Turolla L, Krieger JE, et al. (2014) Presence and type of low density lipoprotein receptor (LDLR) mutation influences the lipid profile and response to lipid-lowering therapy in Brazilian patients with heterozygous familial hypercholesterolemia. Atherosclerosis 233: 206-210.
29. Bertolini S, Pisciotta L, Rabacchi C, Cefalu AB, Noto D, et al. (2013) Spectrum of mutations and phenotypic expression in patients with autosomal dominant hypercholesterolemia identified in Italy. Atherosclerosis 227: 342-348.
30. Guardamagna O, Restagno G, Rolfo E, Pederiva C, Martini S, et al. (2009) The type of LDLR gene mutation predicts cardiovascular risk in children with familial hypercholesterolemia. J Pediatr 155: 199-204 e192.

31. Chaves FJ, Real JT, Garcia-Garcia AB, Civera M, Armengod ME, et al. (2001) Genetic diagnosis of familial hypercholesterolemia in a South European outbreed population: influence of low-density lipoprotein (LDL) receptor gene mutations on treatment response to simvastatin in total, LDL, and high-density lipoprotein cholesterol. J Clin Endocrinol Metab 86: 4926-4932.
32. Fouchier SW, Kastelein JJ, Defesche JC (2005) Update of the molecular basis of familial hypercholesterolemia in The Netherlands. Hum Mutat 26: 550-556.

FIGURE LEGENDS

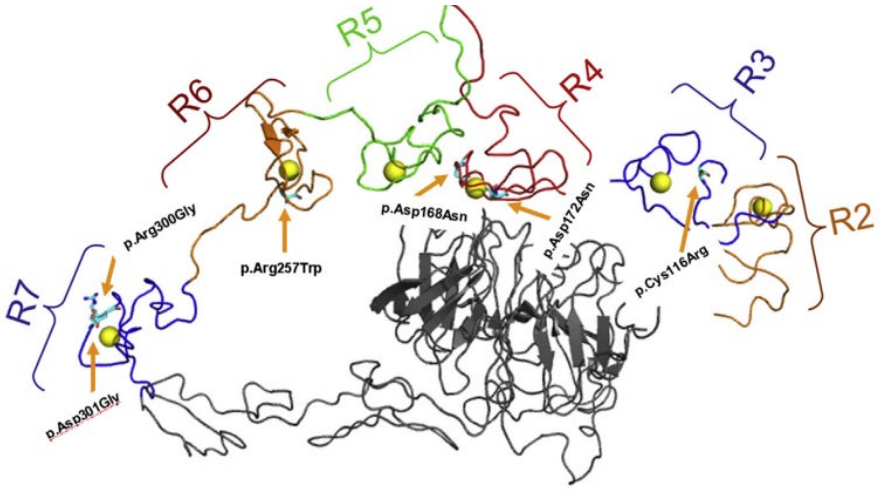

Figure 1: Three-dimensional model of the structure of the LDLR ectodomain from the first cysteine-rich repeat to the EGF domain (black). Location of the variants analysed in this study is shown in each corresponding R module by arrows. This figure was prepared with PyMOL (DeLano scientifics).

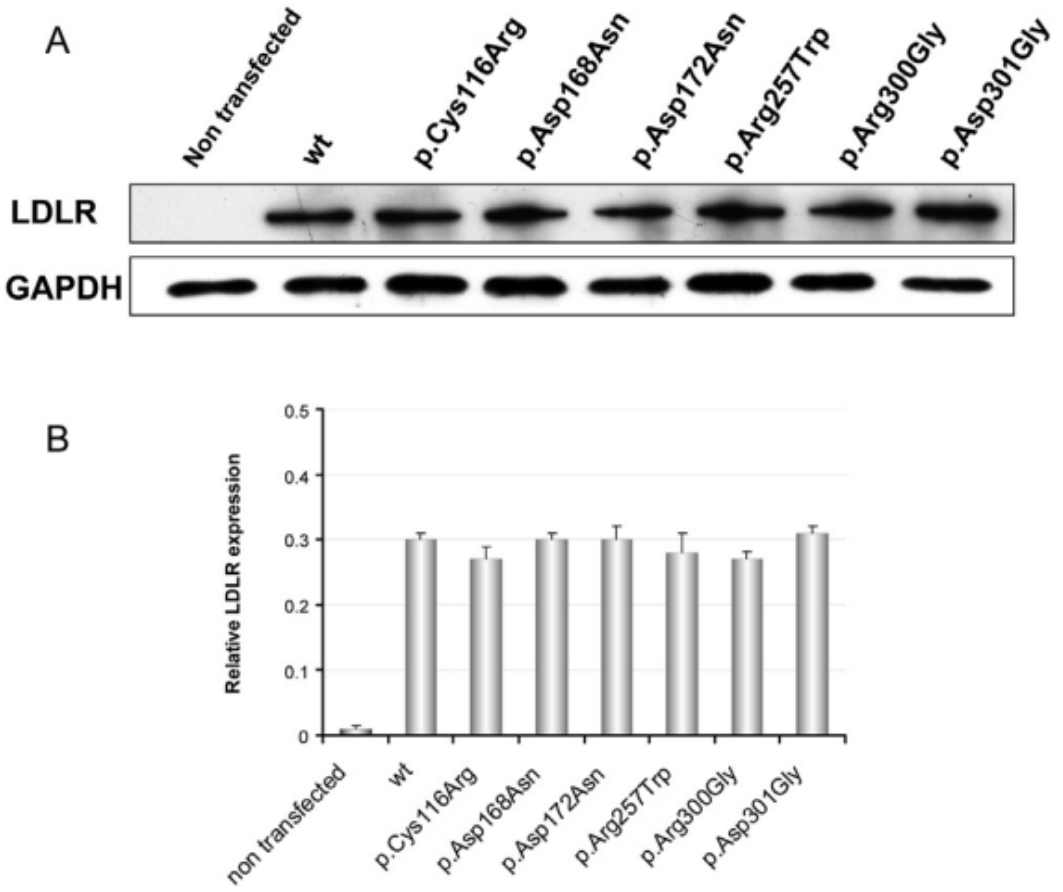

Figure 2: Expression of wt LDLR and LDLR mutations in CHO-*ldlA7* transfected cells. Cells were transfected with the corresponding plasmids carrying the mutations of interest, LDLR was overexpressed for 48 h and then cells were lysed and analysed by Western blot. Whole cell extracts (20 µg) were fractioned in non reducing 8.5% SDS-PAGE, transferred onto nitrocellulose membranes for incubation with a rabbit polyclonal anti-hLDLR antibody and detected by chemioluminiscence as described in Materials and Methods section. The relative band intensity of mature LDLR protein expression was calculated as the ratio of 160 kDa LDLR band intensity to that of GAPDH. A representative experiment from three independently performed assays is shown in upper panel. Levels of significance were determined by a two-tailed Student's t-test, and a confidence level of greater than 95% ($p<0.05$) was used to establish statistical

significance. No statistically significant differences were found among the LDLR expression.

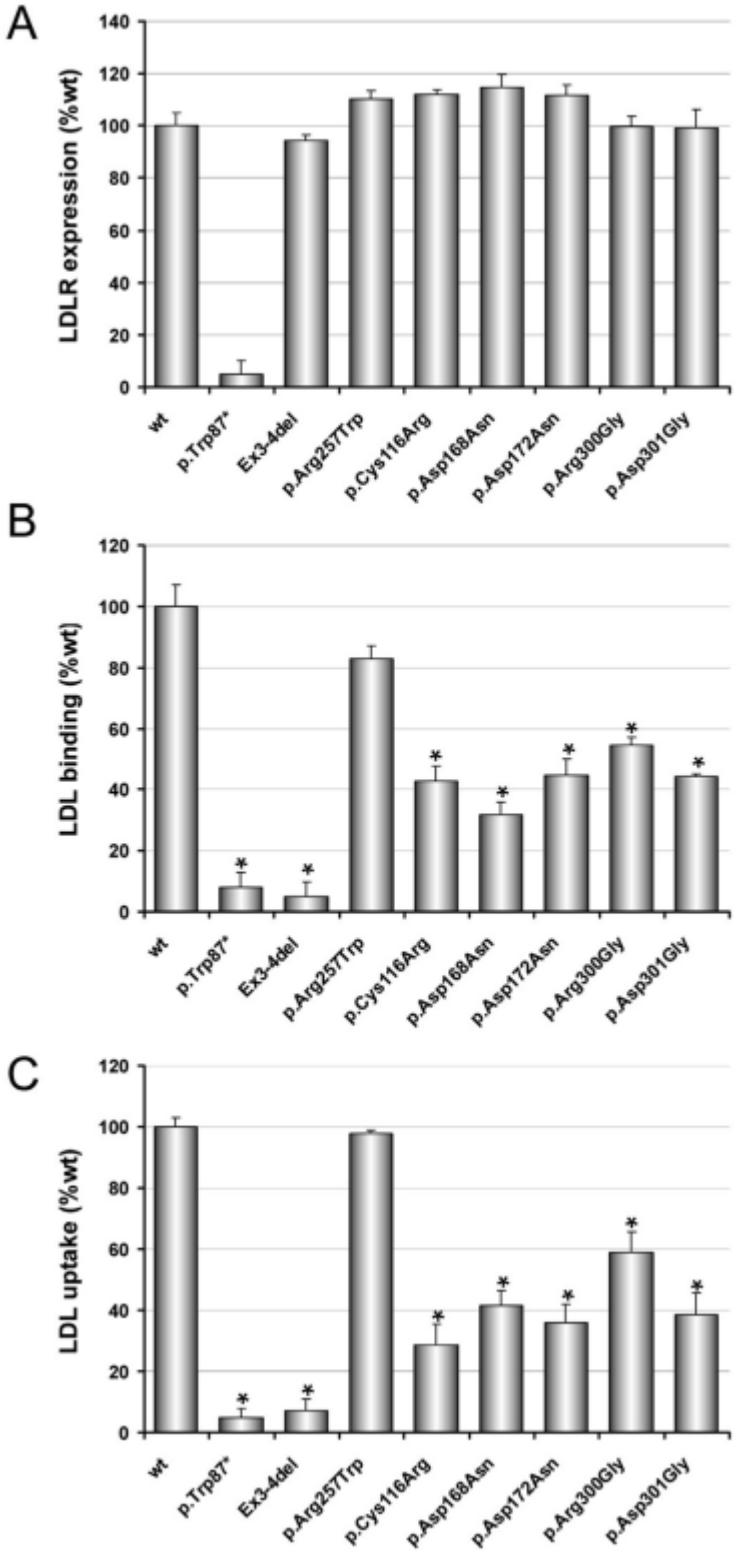

Figure 3: Functional characterization of LDLR variants. A: LDLR expression at cellular membrane; B: LDL-LDLR binding after 4 h incubation at 4 ºC; and C: LDL internalisation efficiency after 4 h incubation at 37ºC. 10,000 cells were acquired in a Facscalibur and values of LDL uptake, binding and LDLR expression were calculated as described in Materials and Methods. The values represent the mean of triplicate determinations (n = 3); error bars represent ±SD. *P < 0.001 compared to the wt using a Student's t-test.

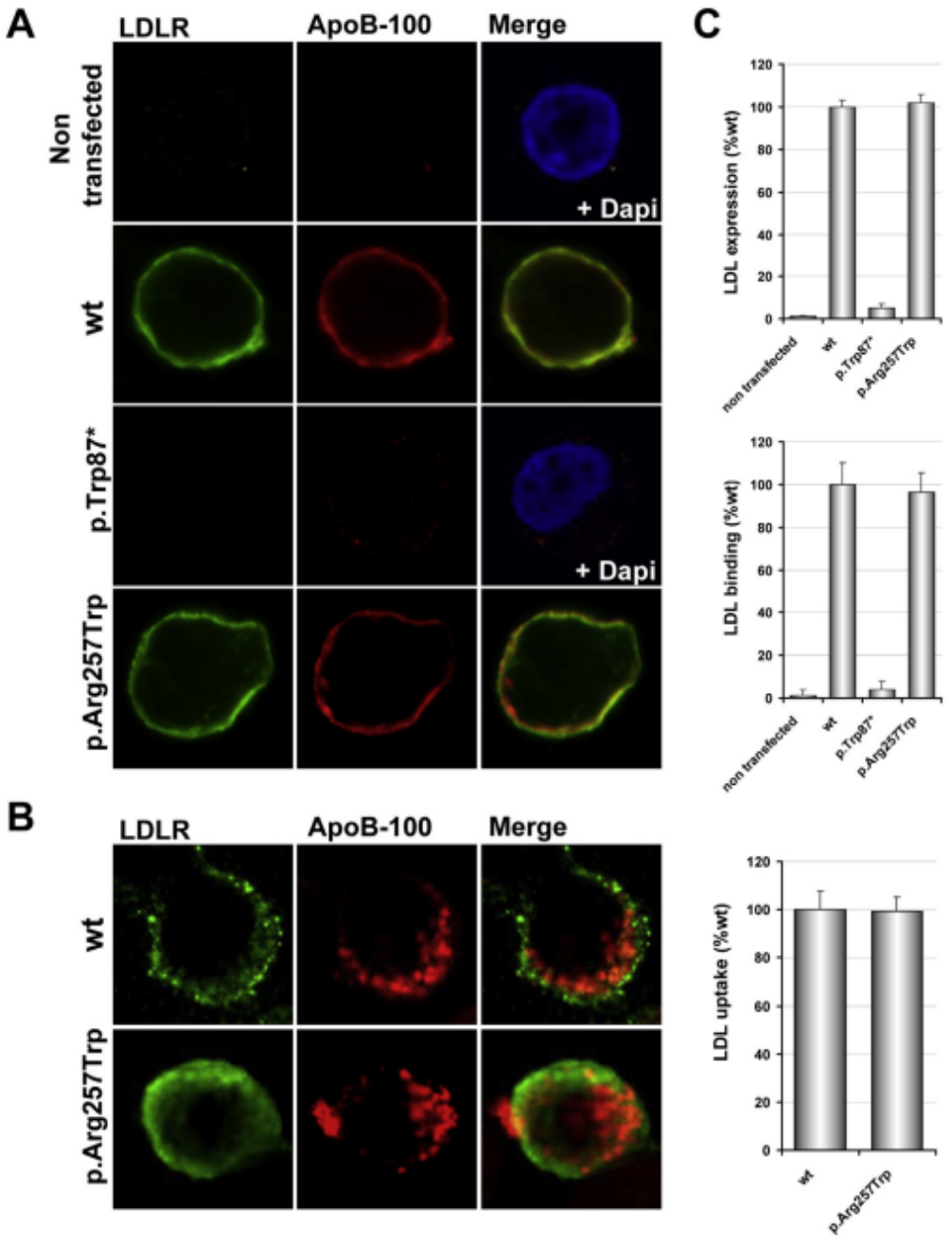

Figure 4: Analysis of wt and p.Arg257Trp LDLR activity by confocal microscopy. A: LDLR expression and LDL binding determined at 4ºC; B: LDL uptake determined at 37ºC; C: Quantification of LDLR expression, LDL binding and LDL uptake in wt and p.Arg257Trp. For LDLR expression and LDL binding assays, transfected cells were incubated with non labelled LDL for 4 h at 4ºC, and for LDL uptake, cells were incubated with non labelled LDL for 4 h at 37ºC as described in Materials and Methods. Anti-

hLDLR and anti-ApoB100 primary antibodies followed by Alexa Fluor® 488 and Texas Red® labelled secondary antibodies were used to visualize LDLR or LDL, respectively. Dapi was used to visualize the nuclei of non transfected cells or p.Trp87* transfected cells. The images show a representative individual cell of n=30. The histograms represent the mean ± standard deviation (n=30 cells), Student's t-test was performed showing no statistical significant differences between wt and p.Arg257Trp.

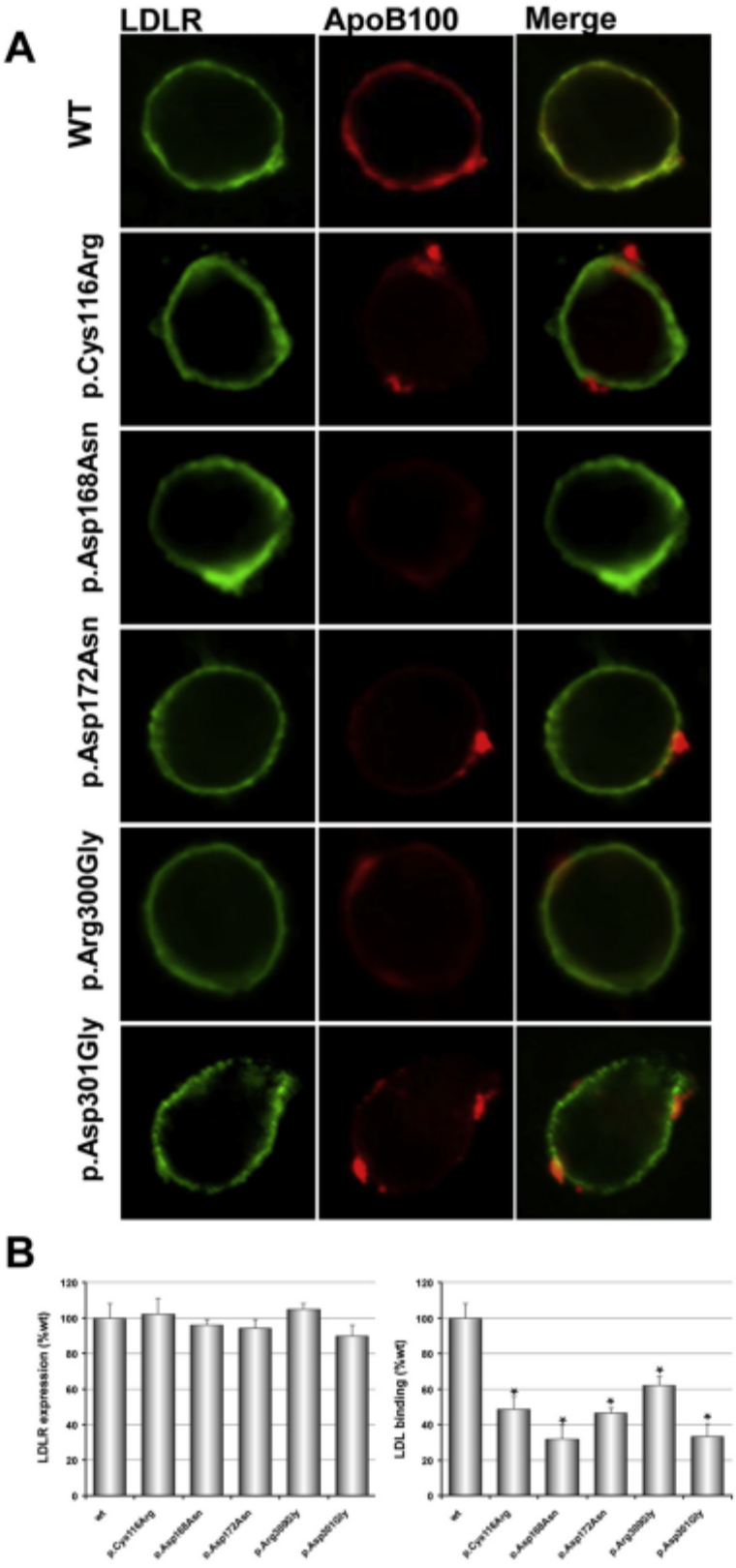

Figure 5: Analysis of LDLR expression and LDL binding in wt, p.Cys116Arg, p. Asp168Ans, p.Asp172Asn, p.Arg300Gly and p.Asp301Gly LDLR variants. A: LDLR

expression and LDL binding determined at 4ºC; B: Quantification of LDLR expression and LDL binding. For LDLR expression and LDL binding assays, transfected cells were incubated with non labelled for 4 h at 4ºC. Anti-hLDLR and anti-ApoB100 primary antibodies followed by Alexa Fluor® 488 and Texas Red® labelled secondary antibodies were used to visualize LDLR or LDL, respectively. The images show a representative individual cell of n=30. The histograms represent the mean ± standard deviation (n=30 cells), *$p < 0.001$ compared to the wild-type (wt) using a Student's t-test.

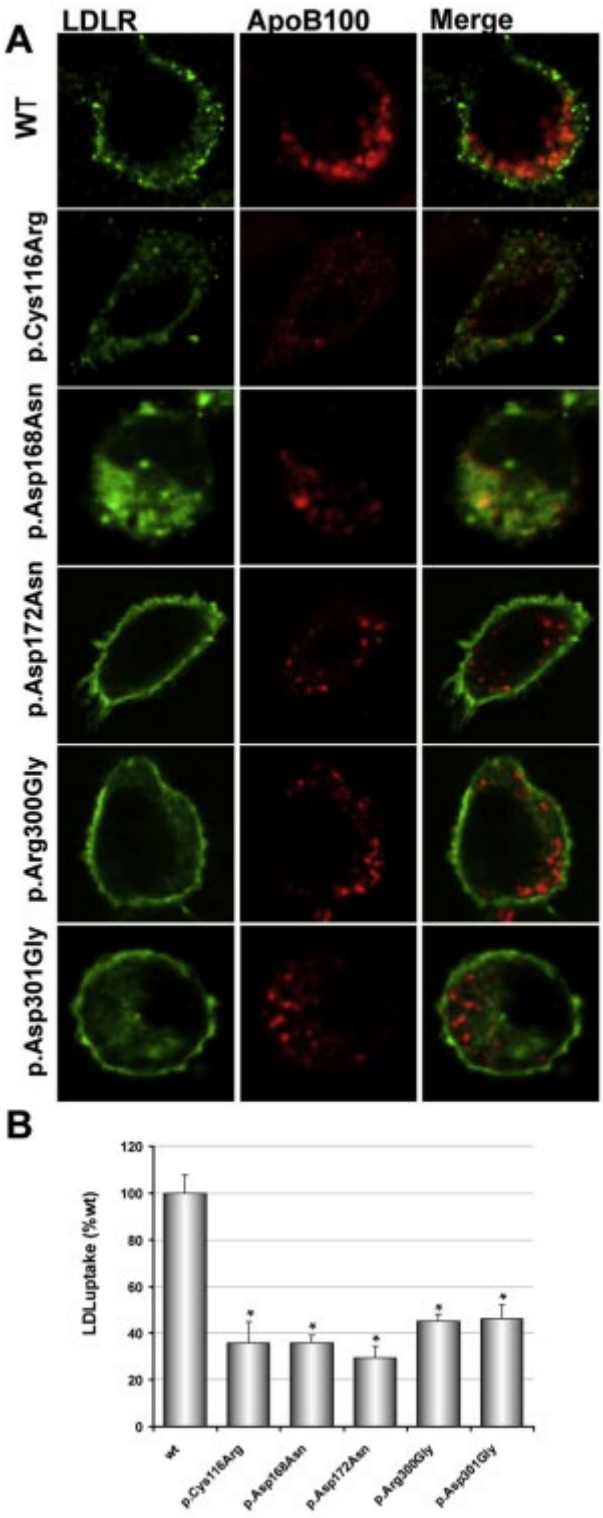

Figure 6: Analysis of LDL uptake in wt, p.Cys116Arg, p. Asp168Ans, p.Asp172Asn, p.Arg300Gly and p.Asp301Gly LDLR variants. A: LDL uptake determined at 37ºC; B: Quantification of LDL uptake. For LDL uptake, cells were incubated with non labelled LDL for 4 h at 37ºC as described in Materials and Methods. Anti-hLDLR and anti-

ApoB100 primary antibodies followed by Alexa Fluor® 488 and Texas Red® labelled secondary antibodies were used to visualize LDLR or LDL, respectively. The images show a representative individual cell of n=30. The histograms represent the mean ± standard deviation (n=30 cells), *p< 0.001 compared to the wild-type (wt) using a Student's t-test.

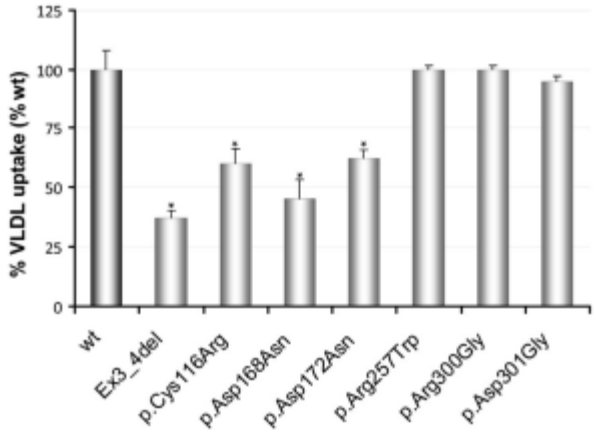

Figure 7: Analysis of VLDL uptake of LDLR variants. VLDL internalisation efficiency was analysed after incubation of transfected cells with FITC-labelled VLDL during 4 h at 37ºC. 10,000 cells were acquired in a Facscalibur and values of VLDL uptake were calculated as described in Materials and Methods. The values represent the mean of triplicate determinations (n = 3); error bars represent ±SD. *P < 0.001 compared to the wt using a Student's t-test.

Supplementary Figure S1: **LDLR expression and LDL binding in wt LDLR and p.Arg257Trp CHO-*ldl*A7 transfected cells.** For LDLR expression and LDL binding assays, cells were incubated with non labelled LDL for 4 h at 4ºC as described in Materials and Methods. Anti-hLDLR and anti-ApoB100 primary antibodies followed by Alexa Fluor® 488 and Texas Red® labelled secondary antibodies were used to visualize LDLR or LDL, respectively.

Supplementary Figure S2: **LDLR expression and LDL binding in wt, p.Cys116Arg, p. Asp168Ans, p.Asp172Asn, p.Arg300Gly and p.Asp301Gly LDLR variants.** For LDLR expression and LDL binding assays, cells were incubated with non labelled LDL for 4 h at 4ºC as described in Materials and Methods. Anti-hLDLR and anti-ApoB100 primary antibodies followed by Alexa Fluor® 488 and Texas Red® labelled secondary antibodies were used to visualize LDLR or LDL, respectively.

Supplementary Figure S3: Structure of the R3 module of the LDLR Binding Domain. (A) Structure of the wt LDLR representing the disulphide bond (yellow arrow), and Ca^{2+} coordination, allowing a correct module conformation. (B) p.Cys116Arg substitution disrupts the disulphide bond. This figure was prepared with PyMOL (DeLano scientifics) (PDB:1N7D).

Supplementary Figure S4: Structure of the R4 module of the LDLR Binding Domain. (A) structure of the wt LDLR representing Asp168 (yellow arrow) and Ca^{2+} coordination, allowing a correct module conformation. (B) p.Asp168Asn substitution on R4 module retains some capacity to interact with calcium (yellow arrow). This figure was prepared with PyMOL (DeLano scientifics) (PDB:1N7D).

Supplementary Figure S5: Structure of the R4 module of the LDLR Binding Domain. (A) Structure of the wt LDLR representing Asp172 (yellow arrow) and Ca^{2+} coordination, allowing a correct module conformation. (B) p.Asp172Asn substitution on R4 module (yellow arrow). This figure was prepared with PyMOL (DeLano scientifics) (PDB:1N7D).

Supplementary Figure S6: Structure of the R7 module of the LDLR Binding Domain. (A) Structure of the wt LDLR representing Asp300 and Arg301 (yellow arrows). (B) p.Asn300Gly substitution (yellow arrow) (C) p.Asn301Gly (yellow arrow). This figure was prepared with PyMOL (DeLano scientifics) (PDB:1N7D).

Table 1: Characteristics of *LDLR* variants included in the study

	Location	cDNA (HGVS)	Protein (HGVS)	LDLR domain	Reference
Positive controls	Exon 3 and 4	c.191-¿_694+?del	p.[L64S];[S65_A232del]	Ligand binding; ΔR2-R4	[9,22]
	Exon 3	c.261G>A	p.W87*	Ligand binding; ΔR2	[23]
Single nucleotide variants	Exon 4	c.346T>C	p.Cys116Arg	Ligand binding; R3	[24]
	Exon 4	c.502G>A	p.Asp168Asn	Ligand binding; R4	[25]
	Exon 4	c.514G>A	p.Asp172Asn	Ligand binding; R4	[26]
	Exon 5	c.769C>T	p.Arg257Trp	Ligand binding; R6	[27,28]
	Exon 6	c.898A>G	p.Arg300Gly	Ligand binding; R7	[29,30]
	Exon 6	c.902A>G	p.Asp301Gly	Ligand binding; R7	[28,31,32]

Table 2: Description of the studied variants, conservation and *in silico* predictions

cDNA (HGVS)	Protein (HGVS)	Nucl. Cons.*	AA Cons.†	Pathogenicity prediction				
				Align GVGD‡	SIFT	Polyphen-2	Mutation Taster	CADD (PHRED value)**
c.346T>C	p.Cys116Arg	1.00	1.00	C65	Not tolerated	Probably damaging (0.999)	Disease causing (p-value: 1.0)	12.28
c.502G>A	p.Asp168Asn	1.00	1.00	C15	Not tolerated	Probably damaging (1)	Disease causing (p-value: 1.0)	12.02
c.514G>A	p.Asp172Asn	1.00	0.92	C15	Not tolerated	Probably damaging (1)	Disease causing (p-value: 1.0)	11.6
c.769C>T	p.Arg257Trp	0.34	0.49	C0	Not tolerated	Probably damaging (0.993)	Polymorphism (p-value: 0.912)	14.07
c.898A>G	p.Arg300Gly	0.69	0.91	C0	Tolerated	Possibly damaging (0.875)	Polymorphism (p-value: 0.925)	0.646
c.902A>G	p.Asp301Gly	0.97	1.00	C65	Not tolerated	Probably damaging (0.999)	Disease causing (p-value: 1.0)	10.16

* Nucleotide conservation.
† Amino acid conservation.
‡ Score values are from C0 (not pathogenic) to C65 (pathogenic).